Response to Referee#1

Thanks to your careful reading and their constructive comments and suggestions on our manuscript. The reviewers' comments and suggestions are shown as *italicized font*, our response to the comments is normal font. New or modified text is in normal font and in blue. Details are as follows.

Referee's comments:

In this study, the authors report on the aqueous OH-initiated oxidation of secondary, primary, and ambient BrC. In the experiments, the authors monitored changes in absorption, using UV-vis spectroscopy, and composition, using high-resolution mass spectrometry, and the experiments appear to have been done carefully. Representatives of primary and secondary BrC were chosen based on the objective of synthesizing the differing rates of photobleaching, known from the literature. The structure of the study and the presentation of the results in figures are generally clear. On the other hand, some of the rationale (e.g., for the choice of secondary BrC) and word choice are not clear. With revisions, the manuscript may be suitable for publication in ACP.

[response]

Thanks for your comments. Please check our point-by-point response.

(1) 1 - The title is suitable and describes an important problem of broad interest to the readers of ACP - note that divergent should be capitalized.

[response]

Thank you for your suggestion. We have revised it.

(2) 19 - Here, alerts should be affects - throughout, there are odd typos and word choices, which I will not list out in detail. A revision for clarity of language is needed.

[response]

We are sorry for these typos. We have carefully revised our manuscript.

(3) 20 - I appreciate the list of the three BrC types here, but a brief clause about the motivation (e.g., to resolve differences in rates of photobleaching in the literature) would be helpful, as well.

[response]

We appreciate reviewer's suggestion. We agree that stating the motivation more explicitly will improve the clarity of the abstract. In fact, the motivation for undertaking this study in the first place is to investigate divergent BrC photobleaching rates (k_{BrC}) reported for different types of BrC in previous studies from molecular perspective. For instance, laboratory experiments proved that representative species of BrC emitted from biomass burning such as 4-nitrocatechol (Hems and Abbatt, 2018) and 2,4-dinitrophenol (Liu et al., 2025) exhibited much lower k_{BrC} than those of aqueous phase reaction-generated secondary BrC (Aiona et al., 2017; Gao and Zhang, 2019). Such differences lead to significant uncertainty in evaluating the evolution of BrC's light absorption capacity in climate models. We have added a brief clause about the motivation for choosing different types of BrC in the revised manuscript.

[revised]
Lines 21-24:

This study investigates and compares photobleaching rates of laboratory-synthesized secondary BrC (aq-BrC), biomass burning-derived BrC (b-BrC), and ambient $PM_{2.5}$-derived BrC (p-BrC) to illustrate the variability in BrC photobleaching kinetics from different types of BrC reported in prior studies.

(4) 32 - I think the abstract should include something about the effort to synthesize the divergent rates here and in the literature (i.e., represented in Fig. 1b).

[response]

Thanks for your suggestion. We agree that integrating a comparison with previous studies into the abstract will better contextualize our findings. In the revised manuscript, we have added relevant results in the abstract that highlights the synthesis of our measured rates with previous studies.

[revised]
Lines 27-28:

Integration of these rate constants with data derived from previous studies highlighted the differences in photobleaching behaviors among BrC from different sources.

(5) 70 - Does the prefix p- stand for primary here? If so, some rationale regarding the absence of secondary BrC in the ambient samples should be provided.

[response]

Thanks for your comments. For the first question, in fact, the prefix "p-" in "p-BrC" stands for "particulate" (derived from ambient $PM_{2.5}$ samples) and not "primary". We have clarified this definition in the revised manuscript to avoid confusion.

For the second question, p-BrC contains a mixture of primary and secondary BrC that is challenging to separate quantitatively. However, the molecular composition of p-BrC based on non-target analysis (NTA) indicates that the p-BrC in this study are predominantly from primary emissions. Table R1 summarizes the sampling details of ambient $PM_{2.5}$ samples. We analyzed the molecular composition of p-BrC samples following the identical approach described in our previous work (Qiu et al., 2024). The detected species were classified into five organic compound groups (acyl compounds (ACs), carboxylic acids (CAs), organonitrates (ONs), nitrophenols (including phenols, NPs), and organosulfates (OSs)) based on elemental composition and MS^2 spectra. Figure R1 shows the molecular composition and relevant solar radiation during sampling, which is represented by the 75th percentile solar radiation (Rad_{75}). As displayed in Table R1 and Figure R1, the sampling occurred predominantly during nighttime or under low Rad_{75}, resulting in minimal photobleaching of p-BrC prior to analysis. In addition, the molecular composition, particularly the presence of nitrophenols, is indicative of primary emissions from sources such as biomass burning and vehicle emissions, rather than secondary formation. We have added a brief rationale in the revised manuscript.

Table R1 Sampling details of ambient $PM_{2.5}$ samples used for p-BrC extraction in this work

Sampling ID	Samping time*	Average $PM_{2.5}$ (μg/m^3)
20201224	10:00–9:00 +1	21.6
20201225	10:00–9:00 +1	27.0
20201226	10:00–9:00 +1	55.6
20201227	10:00–9:00 +1	73.5
20201228	10:00–9:00 +1	42.5

*: All sampling time refers to local time; +1 means the next day

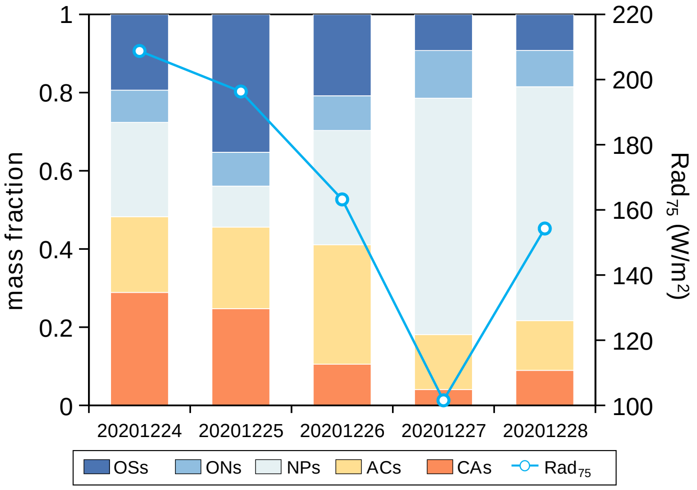

Figure R1 The mass fractions of 5 groups of identified species and Rad_{75} for p-BrC

[revised]

Lines 73-76:

In this work, we performed photochemical aging experiments on three types of BrC under identical, controlled conditions, including synthesized by aqueous phase reaction (referred to “aq-BrC”), and extracted from ambient (referred to “p-BrC”, where “p” denotes particulate) and biomass burning (referred to “b-BrC”) $PM_{2.5}$ samples.

Lines 104-107:

We selected five atmospheric $PM_{2.5}$ samples collected at Peking University Changping Campus (40°8′N, 116°6′E) from 15 December 2020 to 15 January 2021 to extract p-BrC. Table S2 summarizes the sampling time and average $PM_{2.5}$ mass concentrations during sampling of each sample. All samples were collected using a high-volume sampler with the flow rate of 1.05 m^3/min.

Lines 203-210:

It is noteworthy that p-BrC contains a mixture of primary and secondary BrC that is challenging to separate quantitatively. However, from molecular composition and solar radiation during sampling, p-BrC is considered to be predominantly of primary emissions. Herein, we further analyzed the molecular composition of p-BrC following the non-target analysis approach used in our previous study (Qiu et al., 2024), more details were described in Text S2. Figure S4 shows the molecular composition and relevant solar radiation during sampling, which is represented by the 75th percentile solar radiation (Rad_{75}). Low Rad_{75} showed limited photochemical aging prior to analysis, and high mass fraction of nitrophenols proved the dominate role of primary emission for p-BrC.

Table S2:

Same as Table R1.

Figure S5:

Same as Figure R1.

(6) 71 - This is not a particularly compelling way to frame the results - it is well known already that rates for these different types of BrC are different, from the literature.

[response]

Thanks for your comment. We acknowledge that the previous studies contain observations suggesting variable photobleaching kinetics among different types of BrC, like secondary BrC generated via aqueous phase reaction (Aiona et al., 2017; Müller et al., 2023), Suwannee River fulvic acid standard (Borduas-Dedekind et al., 2019), and BrC extracted from biomass burning aerosols (Müller et al., 2023; Wong et al., 2019). However, these prior findings are often fragmented, which are derived from disparate experimental setups, focusing on given BrC types, or reported under non-comparable conditions. This inhibits the establishment of a quantitative, predictive approach linking BrC source to its atmospheric lifetime and global radiative effect.

This work directly addresses this gap by implementing a controlled, comparative experiment to explain and unify the photobleaching kinetic of different types of BrC. Our three key findings are listed as below:

(1) Parametric Approach for Climate Models: We provide directly comparable, pseudo-first-order k_{BrC} for three major BrC types under identical environmental conditions, including steady-state OH concentrations ($[OH]_{ss}$), UV radiation, and concentration of BrC. These identical environmental conditions are crucial because different BrC photobleaching rates reported in previously studies could be conflated with methodological inconsistencies. The divergent k_{BrC} values (varying over an order of magnitude for different types of BrC) establish a clear, source-dependent gradient that can be directly integrated into climate models.

(2) Mechanistic Explanation of the Photobleaching Pathway: Beyond k_{BrC}, we identify and quantify OH oxidation as the dominant pathway (>80% contribution) across all types of BrC. While the importance of OH oxidation is known for some studies (Choudhary et al., 2023), its key and consistent role across different BrC types, demonstrated here through tailored control experiments, simplifies the simulation of BrC photochemical aging in models.

(3) Molecular-Level Linkage from Source to Fate: We used HRMS to trace the evolution of specific BrC chromophores. We show that the divergent k_{BrC} is fundamentally related to distinct molecular composition: the rapid bleaching of aq-BrC is driven by the high OH reactivity of MG and 2-IC oligomers, while the stability of b-BrC is attributable to highly conjugated structures in lignin-derived compounds. This provides a mechanistic explanation for the long-standing observational puzzle of why biomass burning BrC can persist during long-range transport.

[revised]
Lines 76-82:

Compared to previous studies, this work systematically investigated the differences in photobleaching kinetics among various types of BrC under identical environmental conditions. We combine this with high-resolution mass spectrometry (HRMS) analysis to establish a mechanistic link between the observed divergent BrC photobleaching rates and the evolution of key molecular chromophores. In addition, we quantify the contribution of the OH oxidation pathway across all BrC types. These findings aim to provide essential parameters and a mechanistic basis for improving the representation of BrC photochemical aging in climate models.

Line 189-192:

This order-of-magnitude difference in k_{BrC} among three BrC types, quantified under comparable conditions, highlights a fundamental source dependency that cannot be attributed to environmental condition variability. This clear difference necessitates a molecular-level explanation, which we pursue by examining the dominant bleaching pathway and the underlying chemical composition.

(7) 78 - The products of methylglyoxal and ammonium sulfate represent just one sub-type of secondary BrC - another type, e.g., is from the aqueous processing of phenolic precursors. What was the rationale for this choice? I am skeptical that it is a representative choice partly because it is known to photobleach so much faster than ambient secondary BrC.

[response]

We agree that the secondary BrC generated via the reaction between MG and AS represents only one pathway (aldehyde-amine condensation) for secondary BrC formation, and that its notably high photobleaching rate is well-documented. Our rationale for selecting this system was not to claim it as a fully representative surrogate for all ambient secondary BrC, but rather to strategically employ it as a well-defined, representative model compound with a known photochemical reactivity. As we discussed in your last comment, the main aim of this study is to compare photobleaching kinetics across different types of BrC and to explain this difference from molecular-level perspective.

In addition, previous studies have confirmed that MG is one of the most abundant dicarbonyl species in the atmosphere (Gu et al., 2025; Fu et al., 2008). MG is produced by both primary emissions from biofuel and biomass burning, as well as oxidation from VOCs like isoprene, acetone, and alkenes (see (Fu et al., 2008) and references herein). Hence, both anthropogenic and biogenic sources contribute to MG in the atmosphere. MG exhibit a tendency to partition into aqueous aerosols and cloud droplets in the atmosphere (Laskin et al., 2015). Therefore, the secondary BrC generated by the aqueous-phase reaction between MG and AS is representative as aq-BrC.

In the revised manuscript, we have added relevant discussion about the representative and the uncertainty of aq-BrC generated via aqueous-phase reaction between MG and AS.

[revised]

Lines 89-93:

Previous studies have confirmed that MG is one of the most abundant dicarbonyl species in the atmosphere (Gu et al., 2025; Fu et al., 2008), which is produced by primary emissions and oxidation of volatile organic compounds (VOCs). Considering that MG exhibit a tendency to partition into aqueous aerosols and cloud droplets in the atmosphere (Laskin et al., 2015), therefore, the secondary BrC generated by the aqueous-phase reaction between MG and AS is representative as aq-BrC.

(8) 89 - This is where I was expecting some rationale for labelling ambient samples with p- for primary

[response]

Thanks for your comment. We have discussed the meaning of “p” and the contribution of primary emission and secondary formation to p-BrC in the 5th comment. Please check more details in our reply on the 5th comment.

[revised]

Lines 73-76:

In this work, we performed photochemical aging experiments on three types of BrC under identical, controlled conditions, including synthesized by aqueous phase reaction (referred to “aq-BrC”), and extracted from ambient (referred to “p-BrC”, where “p” denotes particulate) and biomass burning (referred to “b-BrC”) $PM_{2.5}$ samples.

Lines 104-107:

We selected five atmospheric $PM_{2.5}$ samples collected at Peking University Changping Campus (40°8′N, 116°6′E) from 15 December 2020 to 15 January 2021 to extract p-BrC. Table S2 summarizes the sampling time and average $PM_{2.5}$ mass concentrations during sampling of each sample. All samples were collected using a high-volume sampler with the flow rate of 1.05 m^3/min.

Lines 203-210:

It is noteworthy that p-BrC contains a mixture of primary and secondary BrC that is challenging to separate quantitatively. However, from molecular composition and solar radiation during sampling, p-BrC is considered to be predominantly of primary emissions. Herein, we further analyzed the molecular composition of p-BrC following the non-target analysis approach used in our previous study (Qiu et al., 2024), more details were described in Text S2. Figure S4 shows the molecular composition and relevant solar radiation during sampling, which is represented by the 75th percentile solar radiation (Rad_{75}). Low Rad_{75} showed limited photochemical aging prior to analysis, and high mass fraction of nitrophenols proved the dominate role of primary emission for p-BrC.

Table S2:

Same as Table R1.

Figure S5:

Same as Figure R1.

(9) 103 - A brief description of how this scaling factor was determined would be helpful.

[response]

Thanks for your suggestion. To estimate the experimental photochemical aging time of BrC under the atmospheric conditions, the photodegradation rate *J* was assumed to be the convolution of spectral flux $F(\lambda)$, quantum yield $\varphi(\lambda)$, and absorption cross section $\sigma(\lambda)$ using eq. (R1):

$$J = \int F(\lambda) \times \varphi(\lambda) \times \sigma(\lambda)\, d\lambda \qquad \text{(R1)}$$

At longer wavelength, the absorption cross section and quantum yield of molecules become small (Malecha et al., 2018). Therefore, limiting the integration to the UV bulb range is reasonable, as photoreactions at longer wavelengths are minimal. For a narrow integration range, the scaling factor can be approximated as the ratio between the integrated spectral flux densities of two different light sources, as shown in eq. (R2):

$$\text{scaling factor} = \frac{\int F(\lambda)_{UV\ bulbs} d\lambda}{\int F(\lambda)_{atmosphere} d\lambda} \qquad \text{(R2)}$$

Using Eq. (R2), the spectral flux densities of the UV bulbs used in this work and the 24-hour average Beijing solar spectrum at 300 m above sea level (typical altitude in Beijing) were integrated from 360 nm to 380 nm. The 24-hour average Beijing solar spectrum was simulated using the Tropospheric Ultraviolet and Visible Radiation model (TUV, https://www2.acom.ucar.edu/modeling/tropospheric-ultraviolet-and-visible-tuv-radiation-model). The setup of the TUV model is listed in Table R2, and the simulated results are displayed in Figure R2. Our calculated results showed that the scaling factor between the experimental exposure and the atmospheric solar exposure was 3.86. In this work, the scaling factor was set to 4.0 to simplify the calculation.

Table R2 Setup of the TUV model

Parameter	Model setup
Latitude	39.92
Longitude	116.33
Date and time	June 20th, 2022

Overhead ozone	300 du
Surface albedo	0.1
Ground altitude	0 km
Measured altitude	0.3 km
Clouds optical depth/base/top	0.00/4.00/5.00
Aerosols optical depth/S-S albedo/alpha	0.235/0.990/1.000
Sunlight direct beam/diffuse down/diffuse up	1.0/1.0/1.0

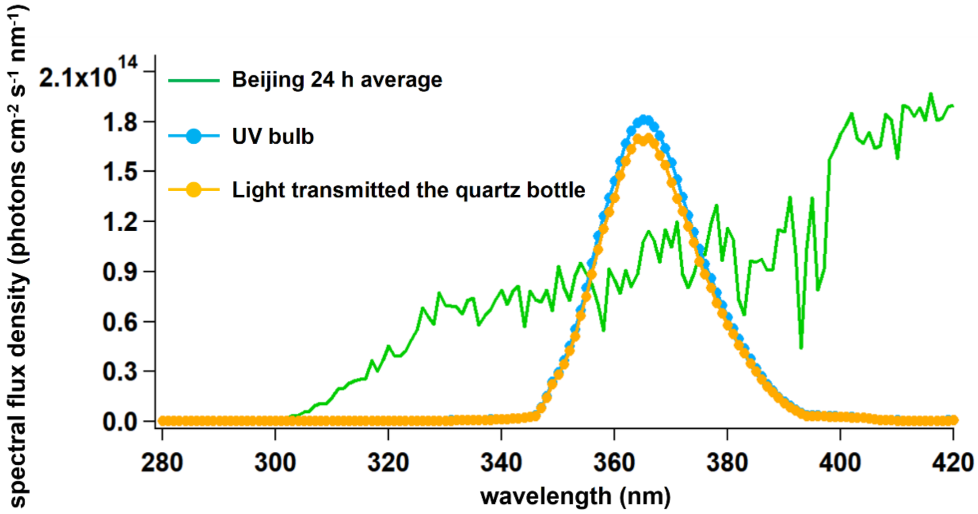

Figure R2 The comparison between the radiation used in laboratory photochemical aging experiment and solar radiation

[revised]

Lines 120-128:

The transition from laboratory experimental illumination to actual solar radiation was applied by calculating the ratio between laboratory and actual spectral flux densities following the identical calculation approach used in our previous study (Qiu et al., 2024). Briefly, the scaling factor can be approximated as the ratio between the integrated spectral flux densities of two different light sources. The spectral flux densities of the UV bulbs used in this work and the 24-hour average Beijing solar spectrum at 300 m above sea level were integrated from 360 nm to 380 nm (see Text S2 for detail). The 24-hour average Beijing solar spectrum was simulated using the Tropospheric Ultraviolet and Visible Radiation model (Table S4), and Figure S3 shows the comparison between calculated and measured radiation spectrum. The calculated scaling factor in this work is 3.86 (Qiu et al., 2024). Samples were collected at 0, 2, 4, 8, and 16 hours of equivalent solar radiation.

Text S2:

To estimate the experimental photochemical aging time of BrC under the atmospheric conditions, the photodegradation rate *J* was assumed to be the convolution of spectral flux $F(\lambda)$, quantum yield $\varphi(\lambda)$, and absorption cross section $\sigma(\lambda)$ using eq. (S1):

$$J = \int F(\lambda) \times \varphi(\lambda) \times \sigma(\lambda)\, d\lambda \qquad (S1)$$

At longer wavelength, the absorption cross section and quantum yield of molecules become small. Therefore, limiting the integration to the UV bulb range is reasonable, as photoreactions at longer wavelengths are minimal. For a narrow integration range, the scaling factor can be approximated as the ratio between the integrated spectral flux densities of two different light sources, as shown in eq. (S2):

$$\text{scaling factor} = \frac{\int F(\lambda)_{UV\ bulbs} d\lambda}{\int F(\lambda)_{atmosphere} d\lambda} \qquad (S2)$$

Using Eq. (R2), the spectral flux densities of the UV bulbs used in this work and the 24-hour average Beijing solar spectrum at 300 m above sea level (typical altitude in Beijing) were integrated from 360 nm to 380 nm. The 24-hour average Beijing solar spectrum was simulated using the Tropospheric Ultraviolet and Visible Radiation model (TUV, https://www2.acom.ucar.edu/modeling/tropospheric-ultraviolet-and-visible-tuv-radiation-model). The setup of the TUV model is listed in Table S3, and the simulated results are displayed in Figure S3. Our calculated results showed that the scaling factor between the experimental exposure and the atmospheric solar exposure was 3.86. In this work, the scaling factor was set to 4.0 to simplify the calculation.

Table S4:

Same as Table R2

Figure S3:

Same as Figure R2.

(10) 135 - It would be helpful to specify that the decay discussed here is the overall decay, rather than the route-specific decays, which are discussed later.

[response]

Thanks for your comment. We have revised accordingly.

(11) 144 - It is not clear to me why the left- and right-hand tick marks are labelled with different numerical values.

[response]

Thanks for your suggestion. In Figure 1(a), the left axis represents the overall decay in ln($MAC_{300,t}$/$MAC_{300,0}$) for p-BrC and b-BrC, while the right axis denotes this decay for aq-BrC. We have added relevant descriptions in the revised manuscript and revised Figure 1(a).

[revised]

Lines 162-163:

The left axis of Figure 1(a) shows the variation in ln($MAC_{300,t}$/$MAC_{300,0}$) for p-BrC and b-BrC, while the right axis denotes this variation for aq-BrC.

Figure 1(a):

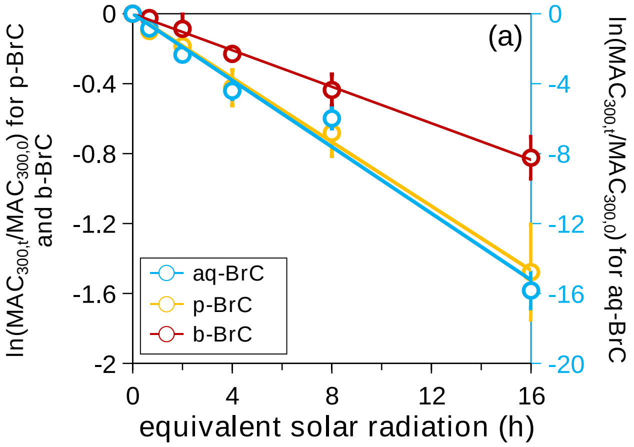

(12) 166 - My perception is that much of the novelty of the study lies in this rough clustering of rates with BrC type.

[response]

Thanks for your comment. The clustering of BrC photobleaching rates by different BrC types, as shown in Figure 1(b), is one of outcome that consolidates data derived from previous studies. However, we need to emphasize that the fundamental novelty of this work extends beyond this clustering to deliver mechanistic understanding from molecular perspective and quantitative parameters. Specifically, our work provides three new insights, as described in our reply to your 6th comment: (1) parametric approach for climate models; (2) mechanistic explanation of the photobleaching pathway; and (3) molecular-level linkage from source to fate.

In summary, this work integrated BrC photobleaching kinetics, mechanism identification, and molecular-level explanation to provide essential parameters and a mechanistic basis for improving the representation of BrC photochemical aging in climate models.

(13) 195 - A table of values of k_BrC; k_BrC,OH; k_BrC,pho; and k_BrC,ctrl would be helpful for clarity. Additional comparisons to route-specific values from the literature are warranted.

[response]

Thanks for your comment. We have added these values in Table 1.

[revised]
Table 1:

BrC type	$k_{BrC,ctrl}$	$k_{BrC,pho}$	$k_{BrC,OH}$
aq-BrC	(0.004±0.002) h^{-1}	(0.19±0.03) h^{-1}	(0.94±0.06) h^{-1}
p-BrC	(0.007±0.001) h^{-1}	(0.02±0.005) h^{-1}	(0.08±0.02) h^{-1}
b-BrC	(0.006±0.002) h^{-1}	(0.01±0.004) h^{-1}	(0.04±0.01) h^{-1}

(14) 198 - The predominant role of OH oxidation is presented here as a central conclusion of this study - some discussion of past studies, which have also shown this role extensively, should be included.

[response]

Thanks for your comment. We fully agree with the reviewer that the important role of OH oxidation in BrC photobleaching has been indicated in several prior studies. This work systematic quantification and comparative verification of its dominate role across three different potential photoblaching pathways under controlled and consistent conditions. While past studies have often focused on and demonstrated the importance of OH oxidation for specific BrC types, like laboratory surrogates or biomass burning BrC, our work provides direct evidence that OH oxidation is the principal pathway (>80% contribution to the overall k_{BrC}) for different BrC types. This result confirms that OH-driven chemistry is a fundamental, unifying driver of BrC photobleaching, regardless of source. Our experimental design, which allowed us to separate the contributions of OH oxidation, direct photolysis, and dark processes. We have revised the manuscript to summarize the prior work and to more clearly frame our contribution in terms of this cross-source quantitative verification.

[revised]
Lines 235-237:

The dominate role of OH oxidation in BrC photobleaching have been also proved in several previous studies (Choudhary et al., 2023; Hems and Abbatt, 2018; Zhao et al., 2015), this work provide quantitative and comparative evidence regardless of BrC types.

(15) 234 - Phenols could also be representative of secondary BrC, if it came from phenolic precursors - an acknowledgement of the variable composition of secondary BrC should be included.

[response]

We agree that phenols could also represent atmospheric secondary BrC. Indeed, phenols and nitrophenols can originate from both primary emissions (e.g., from biomass burning and/or fossil fuel combustion) and secondary formation via the atmospheric oxidation of phenolic VOCs. We fully agree that the composition of secondary BrC is highly variable and can include such aromatic products. In addition, we acknowledge that the photobleaching rates of secondary BrC dominated by phenols are much lower than that of aq-BrC in this work. Specifically, in this work, the measured k_{BrC} of p-BrC, which is dominated by nitrophenols, is an order of magnitude lower than that of aq-BrC. This difference highlights a crucial point, which secondary BrC encompasses a broad range of molecular structures with vastly different k_{BrC}. In the revised manuscript, we have added relevant discussion.

[revised]
Lines 290-295:

It is acknowledged that secondary BrC comprises a wide variety of compounds formed through different pathways. While phenols and nitrophenols identified here can themselves be secondary products, their markedly slower photobleaching rate (compared to the MG/AS-derived aq-BrC in this work) highlights the substantial kinetic diversity within the broader secondary BrC. This further reinforces that the molecular architecture, rather than the primary or secondary classification, is the fundamental determinant of BrC photochemical stability.

(16) 248 - Include here why exact mass concentration cannot be derived (i.e., unknown ionization efficiency and lack of standards).

[response]

The reviewer is correct. The primary reasons why exact mass concentrations cannot be derived directly are indeed the lack of authentic chemical standards for the vast majority of detected compounds. If the mass concentrations of compounds were obtained, a non-target analysis approach based on UHPLC-HRMS should be adopted. This approach relies on standards or surrogate standards. Our goal in this work was to comparatively track the changes in molecular composition for each specific BrC type before and after photobleaching. While absolute quantification is not feasible based on HRMS analysis, the relative changes in signal intensity for a given compound are comparable within the same sample matrix. This is because the matrix effects and ionization conditions were kept identical for the paired “before” and “after” photobleaching of each BrC type. Therefore, the variation in signal intensity for a specific *m/z* can be reliably interpreted as a corresponding change in its relative mass concentration.

[revised]

Lines 333-340:

We noted that the exact variation in the mass concentration of compounds shown in Figure 3 were not derived in this work. Ultra-high performance liquid chromatography (UHPLC)-HRMS analysis using standards or surrogate standards should be adopted to obtain the mass concentration of these compounds. However, this work aims to comparatively track the changes in molecular composition for each specific BrC type before and after photobleaching. While absolute quantification is not feasible based on HRMS analysis, the relative changes in signal intensity for a given compound are comparable within the same sample matrix. Therefore, the variation in signal intensity for a specific *m/z* can be reliably interpreted as a corresponding change in its relative mass concentration.

(17) 265 - Have these species been identified in biomass burning BrC previously? What other studies have investigated BrC from corn straw?

[response]

Thanks for your comment. For your first question, lignin derivatives have been determined as typical species in organic aerosols emitted from biomass burning. In addition, several lignin derivatives like levoglucosan from cellulose, methoxyphenols from lignin have been treated as tracer products of biomass burning aerosols (Simoneit, 2002; Sedlak et al., 2024). Nodakenetin and flavonoids (*m/z* 245.08, 283.06, and 313.07) detected in this work are typical lignin derivatives.

For your second question, corn straw is the most abundant agricultural residue in China. It constitutes approximately 40.0% of the total output from the agricultural products and has an estimated annual production of about 295 million tons. Its resources are highly concentrated in the key agricultural regions of Northeast and North China (e.g., Heilongjiang, Jilin, Shandong, Henan), where its potential for open burning is highest and poses a major concern for regional air quality. (Data from China Statistical Yearbook 2025). Corn straw is recognized as a typical and common domestic biomass fuel in China. A residential biomass burning experiments have shown that BrC from crop residues (like corn straw) can contribute 57-75% to the total light absorption at 375 nm during the burning process (Huang et al., 2022). Therefore, aerosols emitted from corn straw combustion were chosen as typical biomass burning aerosols in this work.

[revised]

Lines 95-99:

Corn straw is recognized as a typical and common domestic biomass fuel in China, constituting approximately 40.0% of the total output from the agricultural products and has an estimated annual production of about 295 million tons. Therefore, $PM_{2.5}$ emitted from corn straw combustion was selected as typical biomass burning aerosols in this work.

(18) 271 - This conclusion is well-known - indeed, it was presented as the motivation for undertaking this study in the first place. I recommend reframing the Conclusion to focus on new insights.

[response]

We fully agree with the reviewer's comment. We have reframed the Conclusion section (Section 4) to forefront the novel insights rather than restating the initial motivation. The revised conclusion will now lead with our core advances: the quantification of photobleaching rate constants of different BrC types, the identification of OH oxidation as the dominant pathway, and the molecular-level explanation linking the rate gradient to the reactivity of specific BrC types.

[revised]
Lines 350-359:

This work quantifies the k_{BrC} for three different types of BrC and demonstrates that their order-of-magnitude differences (aq-BrC > p-BrC > b-BrC) originate from distinct molecular susceptibilities to OH-driven oxidation through controlled comparative experiments. While the source dependency of BrC photobleaching has been suggested, our study mechanistically establishes the linkage between BrC photobleaching kinetics and molecular composition. Specifically, rapid photobleaching of aq-BrC is governed by the high OH reactivity of MG and 2-IC oligomers; in comparison, the remarkable stability of b-BrC is attributed to resilient, conjugated aromatic systems in lignin derivatives. For p-BrC, an intermediate k_{BrC} was observed, consistent with the oxidation kinetics of nitrophenolic chromophores. Critically, we show that OH oxidation accounts for >80% of the total photobleaching across all sources, identifying it as the dominant and unifying chemical pathway under aqueous conditions.

(19) 286 - I recommend acknowledging that even perfect knowledge about the sources of BrC is not enough to accurately predict its climate effects - e.g., impacts of environmental conditions (temperature and relative humidity) are also important.

[response]

We fully agree with the reviewer's comment. We have added the importance of environmental conditions in predicting the climate effect of BrC in the Conclusion and Implications section (Section 4).

[revised]

Lines 366-369:

We should acknowledge that though source-dependent BrC photobleaching rates are essential in assessing BrC's global DRE, the impact of environmental conditions like temperature and relative humidity are also decisive (Schnitzler et al., 2022).

References

Aiona, P. K., Lee, H. J., Leslie, R., Lin, P., Laskin, A., Laskin, J., Nizkorodov, S. A.: Photochemistry of Products of the Aqueous Reaction of Methylglyoxal with Ammonium Sulfate. ACS Earth and Space Chemistry. 1, 522-532. https://doi.org/10.1021/acsearthspacechem.7b00075, 2017.

Borduas-Dedekind, N., Ossola, R., David, R. O., Boynton, L. S., Weichlinger, V., Kanji, Z. A., McNeill, K.: Photomineralization mechanism changes the ability of dissolved organic matter to activate cloud droplets and to nucleate ice crystals. Atmospheric Chemistry and Physics. 19, 12397-12412. https://doi.org/10.5194/acp-19-12397-2019, 2019.

Choudhary, V., Roson, M. L., Guo, X., Gautam, T., Gupta, T., Zhao, R.: Aqueous-phase photochemical oxidation of water-soluble brown carbon aerosols arising from solid biomass fuel burning. Environmental Science: Atmospheres. 3, 816-829. https://doi.org/10.1039/D2EA00151A, 2023.

Fu, T.-M., Jacob, D. J., Wittrock, F., Burrows, J. P., Vrekoussis, M., Henze, D. K.: Global budgets of atmospheric glyoxal and methylglyoxal, and implications for formation of secondary organic aerosols. Journal of Geophysical Research: Atmospheres. 113. https://doi.org/10.1029/2007JD009505, 2008.

Gao, Y., Zhang, Y.: Optical properties investigation of the reactions between methylglyoxal and glycine/ammonium sulfate. Spectrochimica Acta Part A: Molecular and Biomolecular Spectroscopy. 215, 112-121. https://doi.org/10.1016/j.saa.2019.02.087, 2019.

Gu, J., Dutta, S., Sioud, S., Go, B. R., Maity, B., Cavallo, L., Zhang, R., Chan, C. K.: Photoinduced Transformation in Glyoxal- and Methylglyoxal-Ammonium Solutions: Role of Photolysis and Photosensitization. Environmental Science & Technology. 59, 16628-16640. https://doi.org/10.1021/acs.est.5c04889, 2025.

Hems, R. F., Abbatt, J. P. D.: Aqueous Phase Photo-oxidation of Brown Carbon Nitrophenols: Reaction Kinetics, Mechanism, and Evolution of Light Absorption. ACS Earth and Space Chemistry. 2, 225-234. https://doi.org/10.1021/acsearthspacechem.7b00123, 2018.

Huang, R.-J., Yang, L., Shen, J., Yuan, W., Gong, Y., Ni, H., Duan, J., Yan, J., Huang, H., You, Q., Li, Y. J.: Chromophoric Fingerprinting of Brown Carbon from Residential Biomass Burning. Environmental Science & Technology Letters. 9, 102-111. 10.1021/acs.estlett.1c00837, 2022.

Laskin, A., Laskin, J., Nizkorodov, S. A.: Chemistry of Atmospheric Brown Carbon. Chemical Reviews. 115, 4335-4382. https://doi.org/10.1021/cr5006167, 2015.

Liu, Y., Huang, R.-J., Lin, C., Yuan, W., Li, Y. J., Zhong, H., Yang, L., Wang, T., Huang, W., Xu, W., Huang, D. D., Huang, C.: Nitrate-Photolysis Shortens the Lifetimes of Brown Carbon Tracers from Biomass Burning. Environmental Science & Technology. 59, 640-649. https://doi.org/10.1021/acs.est.4c06123, 2025.

Malecha, K. T., Cai, Z., Nizkorodov, S. A.: Photodegradation of Secondary Organic Aerosol Material Quantified with a Quartz Crystal Microbalance. Environmental Science & Technology Letters. 5, 366-371. 10.1021/acs.estlett.8b00231, 2018.

Müller, S., Giorio, C., Borduas-Dedekind, N.: Tracking the Photomineralization Mechanism in Irradiated Lab-Generated and Field-Collected Brown Carbon Samples and Its Effect on Cloud Condensation Nuclei Abilities. ACS Environmental Au. 3, 164-178. https://doi.org/10.1021/acsenvironau.2c00055, 2023.

Qiu, Y., Qiu, T., Wu, Z., Liu, Y., Fang, W., Man, R., Liu, Y., Wang, J., Meng, X., Chen, J., Liang, D., Guo, S., Hu, M.: Observational Evidence of Brown Carbon Photobleaching in Urban Atmosphere at Molecular Level. Environmental Science and Technology Letters. 11, 1032-1039. https://doi.org/10.1021/acs.estlett.4c00647, 2024.

Sedlak, J. A., Vishnoi, M., Forsch, K., Bhadha, P., Aarons, S. M., Grassian, V. H.: Probing Interactions at the Organic–Inorganic Interface of Biomass Burning Aerosol: Reactivity of Organic Tracer Species with Different Iron Oxide Mineral Phases. ACS Earth and Space Chemistry. 8, 2463-2473. 10.1021/acsearthspacechem.4c00212, 2024.

Simoneit, B. R. T.: Biomass burning — a review of organic tracers for smoke from incomplete combustion. Applied Geochemistry. 17, 129-162. https://doi.org/10.1016/S0883-2927(01)00061-0, 2002.

Wong, J. P. S., Tsagkaraki, M., Tsiodra, I., Mihalopoulos, N., Violaki, K., Kanakidou, M., Sciare, J., Nenes, A., Weber, R. J.: Atmospheric evolution of molecular-weight-separated brown carbon from biomass burning. Atmospheric Chemistry and Physics. 19, 7319-7334. https://doi.org/10.5194/acp-19-7319-2019, 2019.

Response to Referee#2

Thanks to your careful reading and their constructive comments and suggestions on our manuscript. The reviewers' comments and suggestions are shown as *italicized font*, our response to the comments is normal font. New or modified text is in normal font and in blue. Details are as follows.

Referee's comments:

The manuscript by Qiu et al. examined the photobleaching kinetics of three types of light-absorbing particles, i.e., aq-BrC, b-BrC, and p-BrC. Results show that aqueous BrC has the fastest decay rate for photobleaching while brown carbon BrC has the lowest decay rate. The authors concluded that such differences were due to different molecular structures of the BrC. For instance, oligomer in aq-BrC samples have a faster reaction rate and degree with OH radicals, while aromatic rings conjugated with oxygen-containing heterocyclic moieties are slower to react with OH radicals, leading to slower decay of absorption for b-BrC. The manuscript reads well and organized, and I recommend the authors address the following comments before publication.

[response]

Thanks for your comments. Please check our point-by-point response.

Major Comments:

In Figure 3, the author listed several major species that showed decay after OH exposure. Are these the top potential BrC species that the author could identify in those samples? What are their signal intensities in the total compounds identified by the HRMS? Are there any other types of BrC species that the author can potentially identify, and what are those other compound's decay percentage?

[response]

Thanks for your comment. These compounds were indeed identified as the most characteristic and reactive BrC species through the following three process:

(1) Differential HRMS analysis: We first calculated differential HRMS spectra of different BrC types before and after 16 hours of solar radiation. Species with a significant negative differential signal intensity (indicating degradation) and an absolute intensity exceeding three times the signal-to-noise ratio (S/N > 3, ensuring higher than detection limit) were selected as candidates significantly affected by photobleaching.

(2) Source-specificity selecting: The candidate lists from the three BrC types were then cross-compared to identify compounds that were highly characteristic of each specific source.

(3) Structural identification: The final shortlisted compounds for each type were subjected to tandem MS analysis. Their chemical structures were inferred by matching the obtained fragmentation patterns in their MS^2 spectra with known reaction pathways and literature data.

Based on these above rules, we obtained the differential HRMS spectra of three BrC types (Figure R1). As for their relative abundance in the total identified compounds, the total signal intensity of these species shown in Figure 3 accounts for 28.1%, 16.4%, and 22.8% of the total identified compounds in aq-BrC, p-BrC, and b-BrC, respectively. While they do not dominate the total organic signal, they are recognized as key light-absorbing chromophores (e.g., nitrophenols, conjugated lignin derivatives, and imidazole oligomers) whose photochemical decay is directly linked to the observed reduction in the MAC. Their decay percentages, as indicated in Figure 3 confirmed their high reactivity and pivotal role in the photobleaching kinetics of their types.

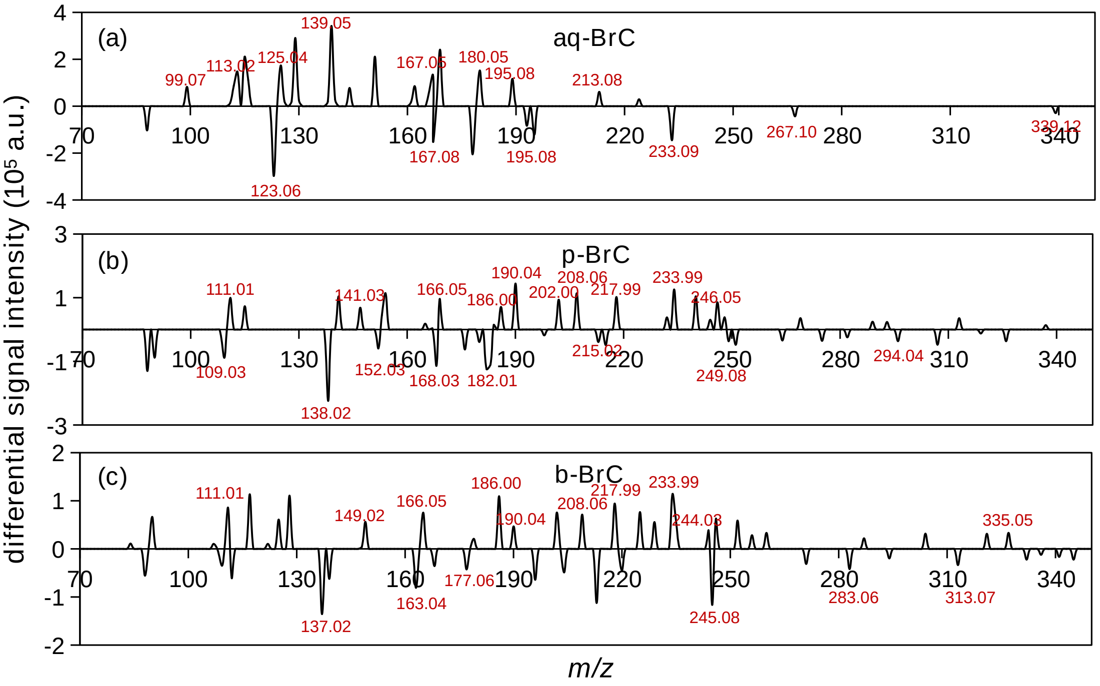

Figure R1 The differential HRMS spectrum of (a) aq-BrC, (b) p-BrC, and (c) b-BrC after 16 hours of solar radiation

As shown in Figure R1, there are several species with negative differential signal intensities. However, their MS^2 spectra were not detected or their chemical structures could not be accurately inferred. Therefore, these species were not shown in Figure 3. In the revised text, we have added relevant discussions.

Furthermore, while the species highlighted in Figure 3 were rigorously selected as representative and reactive chromophores through the differential screening and structural identification process described above, we fully acknowledge that our analysis may not capture all potential BrC chromophores. Limitations in analytical sensitivity, chromatographic separation, and the chemical complexity of BrC mean that some BrC chromophores, particularly those at low concentrations or with poor ionization efficiency, might not be detected or their changes fully characterized. Therefore, while the reported decay percentages for the identified species are robust, the total photobleaching likely involves contributions from additional chromophores not specifically tracked here. In the revised manuscript, we have added relevant discussion to explain this uncertainty.

[revised]

Lines 277-283:

Subsequently, we determined representative BrC chromophores relate to the photobleaching of different types of BrC based on the following three criteria. Firstly, we calculated the differential HRMS spectra of different types of BrC before and after photobleaching (Figure S6). These peaks with negative intensities (> 3 times the signal-to-noise ratio) denote species consumed after photobleaching. Secondly, these candidate species were cross-compared to identify compounds that were highly characteristic of each specific source. Lastly, tandem HRMS (HRMS^2) analysis was adopted to determine the chemical structure of selected BrC chromophores.

Lines 341-348:

In addition, while the species highlighted in Figure 3 were rigorously selected as representative and reactive chromophores through the differential screening and structural identification process described above, we fully acknowledge that our analysis may not capture all potential BrC chromophores. Limitations in analytical sensitivity, chromatographic separation, and the chemical complexity of BrC result in several BrC chromophores, particularly those at low concentrations or with poor ionization efficiency, might not be detected or their changes fully characterized. Therefore, while the reported decay percentages for the identified species are robust, the total BrC photobleaching likely involves contributions from additional chromophores not specifically tracked here.

One of the major assumptions that the author has is about pseudo-first order reaction between BrC and OH radicals in those experiments, but I wonder whether this assumption stands. Would it be possible that, the slower reaction of b-BrC with OH was not due to the molecular structure, but more because of other non-light-absorbing species competing with BrC to react with OH? For instance, for b-BrC samples, *levoglucosin often accounts for a large mass ratio, and it may react with OH radicals predominantly, to slow down the reaction of other BrC molecules reacting with OH. How does the author explain these?*

[response]

Thanks for your comment. As for the pseudo-first-order kinetics, this assumption holds under our experimental conditions where the $[OH]_{ss}$ was maintained constant and in excess compared to the concentrations of individual BrC chromophores. The linear decay of $\ln(MAC_{300})$ over time for all BrC types (Figure 1(a) in the main text) strongly supports that the overall photobleaching follows pseudo-first-order kinetics with respect to the light-absorbing ensemble, consistent with numerous previous studies (Hems and Abbatt, 2018; Choudhary et al., 2023).

As for the potential effect of the reaction between levoglucosin and OH radicals, we agree that the reviewer's comment is plausible. However, our experimental design and molecular-level evidence suggest that while such a phenomenon may occur, the chemical stability of the key BrC chromophores is the dominant factor.

Firstly, **the mass concentration of BrC is controlled in this work**. All photobleaching experiments were conducted with solutions normalized to the same TOC mass concentration (50 mgC/L). This standardization equalized the total potential OH sinks across different BrC types, making the observed order-of-magnitude difference in k_{BrC} more likely attributable to the reactivity of the chromophores themselves rather than solely to differences in competitor abundance.

Secondly, **the molecular evidence for chemical stability of b-BrC is provided by our HRMS results**. The identified lignin derivatives (e.g., flavonoids, nodakenein) exhibited low signal decay percentages (<50%, see Figure 3(c) in the main text) despite being exposed to the same $[OH]_{ss}$ as the highly reactive aq-BrC chromophores. If the slow photobleaching of b-BrC were primarily due to competitive OH scavenging by levoglucosin, we would not expect to see such a strong correlation between specific, conjugated molecular structures and low decay rates. The fact that these stable structures are selectively preserved points to their intrinsic low reactivity.

While levoglucosan is a major mass component in biomass burning aerosol, its own reaction with OH is relatively slow (lifetime of several days in the aqueous phase). Its primary role is likely as a stable tracer or precursor for secondary processes, rather than as a dominant, fast OH sink that would drastically shield chromophores over our experimental timescale.

In conclusion, we agree that the existence of levoglucosan may influence the measured k_{BrC} for b-BrC. However, the consistency between the low observed k_{BrC} for b-BrC, the low decay percentages of its highly conjugated chromophores under controlled $[OH]_{ss}$, and the established chemical stability of such structures strongly supports the conclusion that molecular architecture is the principal determinant of its photobleaching resistance. We have added relative discussion acknowledging the potential modulating role of non-chromophoric OH sinks while reiterating the evidence for intrinsic stability.

[revised]
Lines 325-332:

However, studies found that levoglucosan, which is an important component in biomass burning aerosols, may be oxidized by OH radicals and therefore slow down the reaction of other BrC chromophores reacting with OH. In this work, the same TOC mass concentrations (50 mg/L) across all BrC types provides equal total potential OH sinks, making the observed order-of-magnitude difference in k_{BrC} more likely attributable to the reactivity of the chromophores themselves rather than solely to differences in competitor abundance. Additionally, the identified lignin derivatives exhibited low signal decay percentages despite being exposed to the same $[OH]_{ss}$ as the highly reactive BrC chromophores. Hence, it is expected that the chemical stability of lignin derivative leads to the low k_{BrC} for b-BrC.

Lastly, the aq-BrC was lab-generated with relatively simple ingredients, while p-BrC and b-BrC were collected from ambient samples. The author should discuss potential overcomplications of aq-BrC, and how this would affect the results interpretation.

[response]

We appreciate reviewer's suggestion. We fully acknowledge that our lab-generated aq-BrC (MG+AS system) represents a simplified model of atmospheric aqueous-phase chemistry, lacking the immense molecular diversity and potential matrix effects (e.g., inorganic ions, metals, other organics) present in real aerosol liquid water. However, our rationale for selecting this system was not to claim it as a fully representative surrogate for all ambient secondary BrC, but rather to strategically employ it as a well-defined, representative model compound with a known photochemical reactivity.

By using a system with well-defined precursors and known major products (e.g., imidazole oligomers), we could unambiguously trace the photochemical reaction of specific BrC chromophores and establish a clear cause-and-effect relationship: molecules with high chemical reactivity lead to extremely rapid OH oxidation-driven photobleaching. This establishes a foundational chemical principle. In addition, aq-BrC provides a controlled, high-reactivity system in our experiment. The order-of-magnitude difference between aq-BrC and b-BrC is not interpreted to mean that atmospheric aqueous chemistry always photobleaches this fast, but rather that the aq-BrC shows high potential photoreactivity in the atmosphere. The much slower rates observed for p-BrC and b-BrC must therefore be due to intrinsic molecular stability.

However, we acknowledge that the absolute k_{BrC} value for aq-BrC measured in this work should not be directly extrapolated to all atmospheric secondary BrC. However, the relative ranking of k_{BrC} (aq-BrC >> p-BrC > b-BrC) and, more importantly, the mechanistic insights gained (OH dominance, structure-reactivity relationship) are applicable in the atmosphere. In summary, the stability of atmospheric BrC (especially b-BrC) can be understood as arising from chromophores that are structurally more akin to stable species.

In the revised manuscript, we have added more discussion to explicitly acknowledge this limitation and to clarify that our aq-BrC results illustrate a key reactive pathway and its structural determinants.

[revised]
Lines 241-246:

It is important to note that the laboratory-synthesized aq-BrC represents a simplified chemical system. While it provides a clear mechanistic understanding of rapid photobleaching driven by BrC chromophores with high chemical reactivity, real atmospheric aqueous-phase processes involve more complex precursors and mixtures, yielding secondary BrC with different photobleaching kinetics. Nevertheless, the dominate role of OH oxidation established in this work, which provides a critical lens through which to interpret the slower photobleaching rates of the more complex ambient (p-BrC) and biomass burning (b-BrC) samples.

Lines 290-295:

It is acknowledged that secondary BrC comprises a wide variety of compounds formed through different pathways. While phenols and nitrophenols identified here can themselves be secondary products, their markedly slower photobleaching rate (compared to the MG/AS-derived aq-BrC in this work) highlights the substantial kinetic diversity within the broader secondary BrC. This further reinforces that the molecular architecture, rather than the primary or secondary classification, is the fundamental determinant of BrC photochemical stability.

Minor Comments:

Can the author list the absolute MAC300 values of each type of BrC before phtobleaching? I only see the normalized MAC300 values.

[response]

Thanks for your suggestion. We have added MAC_{300} values of BrC in the revised manuscript.

[revised]

Lines 159-160:

The measured MAC_{300} of aq-BrC, p-BrC, and b-BrC is $(7.32\pm0.89) \times 10^3$ cm^2 g^{-1}, $(7.38\pm0.83) \times 10^2$ cm^2 g^{-1}, and $(9.44\pm0.71) \times 10^3$ cm^2 g^{-1}, respectively.

Some references have DOI and others do not. Please try to keep the formatting the same.

[response]

Revised.

References

Choudhary, V., Roson, M. L., Guo, X., Gautam, T., Gupta, T., Zhao, R.: Aqueous-phase photochemical oxidation of water-soluble brown carbon aerosols arising from solid biomass fuel burning. Environmental Science: Atmospheres. 3, 816-829. https://doi.org/10.1039/D2EA00151A, 2023.

Hems, R. F., Abbatt, J. P. D.: Aqueous Phase Photo-oxidation of Brown Carbon Nitrophenols: Reaction Kinetics, Mechanism, and Evolution of Light Absorption. ACS Earth and Space Chemistry. 2, 225-234. https://doi.org/10.1021/acsearthspacechem.7b00123, 2018.